Inorganic Chemistry
Article

Inorg. Chem. **2010**, *49*, 3183–3191 **3183**
DOI: 10.1021/ic902059y

Conformationally Modulated Intramolecular Electron Transfer Process in a Diaza[2,2]ferrocenophane

Francisco Otón,[†] Imma Ratera,[†] Arturo Espinosa,[‡] Alberto Tárraga,[‡] Jaume Veciana,*[,†] and Pedro Molina[‡]

[†]*Molecular Nanoscience and Organic Materials Department, Institut de Ciència de Materials de Barcelona (CSIC)/CIBER-BBN, Campus Universitari de Bellaterra, E-08193, Cerdanyola, Spain, and* [‡]*Universidad de Murcia, Departamento de Química Orgánica, Facultad de Química, Campus de Espinardo, E-30100 Murcia, Spain*

Received October 17, 2009

A novel conformationally modulated Intramolecular Electron Transfer (IET) phenomenon has been observed due to the cyclic structure of the diaza[2.2]ferrocenophane **3**. The corresponding mixed-valence compound of **3**, prepared by electrochemical or chemical partial oxidation, interestingly shows the appearance of two absorption bands in the near infrared (NIR) spectral region. These bands are attributable to two intervalence charge-transfer transitions associated to two atropoisomers exhibiting different energy for the IET process. A solvent and temperature control over the atropoisomeric equilibrium have also been observed. The experimental data and conclusions about both the conformational and the electronic properties of compound **3** are also supported by density functional theory calculations.

Introduction

Homo- and heterobinuclear complexes with π-conjugated bridges have attracted considerable attention during recent years because they serve as simple models for investigating metal−metal electronic communication.[1] Understanding and controlling the factors governing the Intramolecular Electron Transfer (IET) processes has long been an important pursuit in physical chemistry (i.e., the research of Marcus, Hush, and others) mainly because of the interest in the possible applications for molecular electronic devices.[2] Although it has been extensively studied how the nature of the bridge constitutes a dominant factor in determining the magnitude of the of IET phenomena between redox centers, the effect of the molecular torsions between the donor and the acceptor units has been less studied. Recent works have demonstrated that stereochemical influences provide a significant contribution to the barrier to intramolecular electron transfer, and indeed are manifested in the IET properties of the system.[3] Moreover, the conformational modulation of intramolecular electron transfer processes in biomolecules, fundamentally proteins, is also under study because of the importance that this phenomenon can represent in the understanding of biological mechanisms like photosynthesis and respiration.[4]

It is also known that cyclic and conformationaly constrained structures like cyclophanes can present more than one stable conformer, and the interconversion barriers strongly depend of the nature and length of the bridges.[5] In this context, ferrocenophanes are cyclic compounds that present a particular conformational behavior because of the free rotation of the Cp rings of the ferrocene unit. Ferrocene systems have been attractive candidates for studying mixed-valence behavior, since ferrocene has a well-developed organic chemistry, allowing attachment to a wide variety of bridges, high stability in both the oxidized and neutral states, and charge-transport ability. There is also an increasing awareness that such metal capped π-conjugated systems will play a role in the design of new generations of electronic materials[6] and many studies on linked bis(ferrocenyl) compounds have been

*To whom correspondence should be addressed. E-mail: vecianaj@icmab.es.

(1) (a) Paul, F.; Lapinte, C. *Coord. Chem. Rev.* **1998**, *431*, 178–180. (b) Schwab, P. F. H.; Levin, M. D.; Michl, J. *Chem. Rev.* **1999**, *99*, 1863–1934. (c) Wheatley, N.; Kalck, P. *Chem. Rev.* **1999**, *99*, 3379–3420. (d) Balzani, V.; Juris, A.; Venturi, M.; Campagna, S.; Serroni, S. *Chem. Rev.* **1996**, *96*, 759–834.

(2) (a) Joachim, C.; Gimzewski, J. M.; Aviram, A. *Nature* **2000**, *408*, 541–548. (b) Tour, J. M. *Acc. Chem. Res.* **2000**, *33*, 791–804. (c) Carroll, R. L.; Gorman, C. B. *Angew. Chem., Int. Ed.* **2002**, *41*, 4378–4400.

(3) (a) D'Alessandro, D. M.; Kelso, L. S.; Keene, F. R. *Inorg. Chem.* **2001**, *40*, 6841–6844. (b) D'Alessandro, D. M.; Keene, F. R. *New. J. Chem.* **2006**, *30*, 228–237. (c) Rosokha, S. V.; Sun, D.-L.; Kochi, J. K. *J. Phys. Chem.* **2002**, *106*, 2283–2292.

(4) (a) Croney, J. C.; Helms, M. K.; Jameson, D. M.; Larsen, R. W. *Biophys. J.* **2003**, *84*, 4135–4143. (b) Ji, H.; Yeh, S.-R.; Rousseau, D. N. *J. Biol. Chem.* **2004**, *279*, 9392–9399. (c) Larsen, R. W.; Omdal, D. H.; Jasuja, R.; Niu, S. L.; Jameson, D. M. *J. Phys. Chem. B* **1997**, *101*, 8012–8020.

(5) (a) Gibson, H. W.; Wang, H.; Chang, C. P.; Glass, T. E.; Schoonover, D.; Zakharov, L. N.; Rheingold, A. L. *Heteroat. Chem.* **2008**, *19*, 48–54. (b) Conejo-García, A.; Campos, J. M.; Entrena, A.; Sánchez-Martín, R. M.; Gallo, M. Á.; Espinosa, A. *J. Org. Chem.* **2003**, *68*, 8697–8699.

(6) (a) Tour, M. J. *Acc. Chem. Res.* **2000**, *33*, 791–804. (b) Robertson, N.; McGowan, C. A. *Chem. Soc. Rev.* **2003**, *32*, 96–103. (c) Casado, J.; Rodriguez Gonzalez, S. A.; Ruiz Delgado, M. C.; Moreno Olivas, M.; López Navarrete, J. T.; Caballero, R.; de la Cruz, P.; Langa, F. *Chem.—Eur. J.* **2009**, *15*, 2548–2559.

Published on Web 03/08/2010

reported and comprehensively reviewed.[7] The physical properties of rigid-rod π-conjugated molecules such as biferrocenes **I** and ferrocenophanes **II** are determined predominantly by the extent of delocalization and by electronic interactions between the iron centers. It has been shown that the relative small structural change in going from biferrocenes **I** to ferrocenophanes **II** produces a drastic difference in the physical properties of the mixed valence (MV) compounds.[8] Despite of the rich chemistry of ferrocene, [m.n]ferrocenophanes type **II** bridged by nitrogen-containing chains remains almost unexplored, and only recently have the preparation and properties of two multinuclear nitrogen-rich [4.4] and [3.3] ferrocenophanes been reported.[9]

Taking into account all the above comments, a simple molecule with more than one intramolecular electron transfer process showing multiple near infrared (NIR) absorption bands whose energy could be modified conformationally would be of special interest both theoretically and for the design of new switchable NIR emitters to be used,that is, in short-range telecommunications, among other applications.[10]

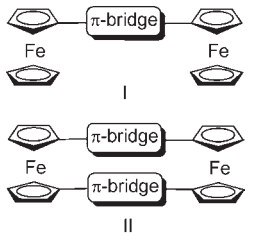

Block 1

In this paper, we describe the preparation of a multinuclear [2.2]ferrocenophane linked by an aza-unsaturated chain in the guise of an aldiminic functionality that because of its rigidity presents two stable conformers, each one presenting different IET energies. The thermal interconversion of the two isomers gives place, as far as we know, to the first example of a MV compound with two IET bands caused by two different conformers that can interconvert. We will also investigate theoretically the effect of molecular conformation on orbital energy levels for the understanding of the variation of the electron-transfer energies.

Results and Discussion

Synthesis and Characterization. Preparation of the target [2.2]metallocenophane is achieved starting from

Scheme 1

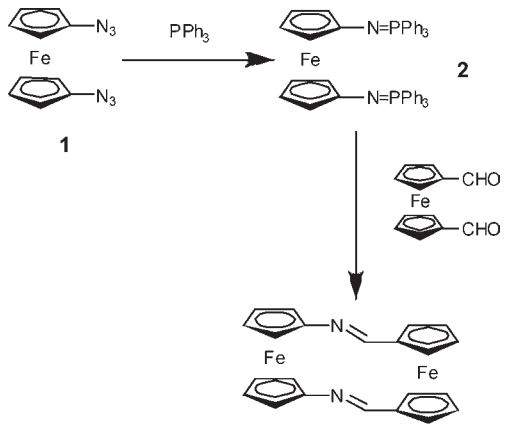

the bis(iminophosphorane) 1,1′-bis(*N*-triphenylphosphoranylidenamino)ferrocene **2**, readily available by a Staudinger reaction with triphenylphosphine of 1,1′-bis(azido)-ferrocene.[11] Bis(iminophosphorane) **2** displays the typical reactivity showed by monoiminophosphoranes in aza-Wittig-type reactions toward carbonyl compounds.[12] Thus, an aza-Wittig reaction with equimolecular amounts of 1,1′-diformylferrocene provided the bis(aldimine)ferrocene **3** in a 72% yield (Scheme 1). The structure of the [2.2]metallocenophane was determined by means of standard spectroscopic techniques (IR, ^{1}H and ^{13}C NMR), mass spectrometry, and elemental analyses, all data being in agreement with the proposed structures.

The presence of two differentiated ferrocene moieties in the [2.2]ferrocenophane **3** is clearly revealed from the analysis of its ^{1}H NMR spectrum. Thus, while a singlet at δ = 9.39 ppm is observed for the iminic protons within the asymmetric imine bridges, four different signals (H_α = 4.07, $H_{\alpha'}$ = 4.24, H_β = 5.12, and $H_{\beta'}$ = 5.44 ppm) are observed, which are associated to the two different monosubstituted Cp rings belonging to both ferrocene subunits.

Electrochemical studies were carried out using cyclic voltammetry (CV). The CV response of compound **3** in CH_2Cl_2, containing 0.1 M [*n*-Bu_4N]PF_6 (TBAHP) as supporting electrolyte, showed two electrochemically reversible one-electron waves at $E_{1/2}$ = −0.06 V and $E_{1/2}$ = 0.45 V vs ferrocene/ferrocenium (Fc^+/Fc) redox couple corresponding to the redox processes of the two ferrocene moieties (see Supporting Information). To assign each redox processes to the corresponding ferrocene moiety, and taking into account that in terms of electron-donating capability the *p*-methoxyphenyl moiety is very similar to the ferrocene, as demonstrated experimentally by absorption spectroscopy, nonlinear optical and electrochemical measurements,[13] the aldimines **4** and **5** were synthesized, and their electrochemical data have been used for comparison purposes. Compounds **4** and **5** exhibit reversible oxidation waves at $E_{1/2}$ = 0.22 V and $E_{1/2}$ = −0.07 V vs Fc^+/Fc, respectively. On the basis of

(7) (a) Cannon, R. D.; White, R. P. *Prog. Inorg. Chem.* **1988**, *36*, 195–298. (b) Manners, I. *Angew. Chem., Int. Ed. Engl.* **1996**, *35*, 1620–1621. (c) Groβman, B.; Heinze, J.; Herdtweg, E.; Kohler, F. H.; Nöth, H.; Schwenk, H.; Spiegler, M.; Wachter, W.; Weber, B. *Angew. Chem., Int. Ed. Engl.* **1997**, *36*, 387–389. (d) Hissler, M.; El-Gharyoury, A.; Harriman, A.; Ziessel, R. *Angew. Chem., Int. Ed.* **1998**, *37*, 1717–1720. (e) Demadis, K. D.; Hartshorn, C. M.; Meyer, T. J. *Chem. Rev.* **2001**, *101*, 2655–2686.

(8) (a) Barlow, S.; O'Hare, D. *Chem. Rev.* **1997**, *97*, 637–670. (b) Ceccon, A.; Santi, S.; Orian, L.; Bisello, A. *Coord. Chem. Rev.* **2004**, *248*, 683–724. (c) Warratz, R.; Aboulfadl, H.; Bally, T.; Tuczek, F. *Chem.—Eur. J.* **2009**, *15*, 1604–1617.

(9) (a) Caballero, A.; Lloveras, V.; Tárraga, A.; Espinosa, A.; Velasco, M. D.; Vidal-Gancedo, J.; Rovira, C.; Wurst, K.; Molina, P.; Veciana, J. *Angew. Chem., Int. Ed.* **2005**, *44*, 1977–1981. (b) Otón, F.; Tárraga, A.; Molina, P. *Org. Lett.* **2006**, *8*, 2107–2110. (c) Otón, F.; Espinosa, A.; Tárraga, A.; Ramírez de Arellano, C.; Molina, P. *Chem.—Eur. J.* **2007**, *13*, 5742–5752.

(10) (a) Ward, M. D. *J. Solid State Electrochem.* **2005**, *9*, 778–787. (b) Lin, C.-Y.; Huang, S-C; Chen, Y.-C. *Electrochem. Commun.* **2008**, *10*, 1411–1414.

(11) Tárraga, A.; Otón, F.; Espinosa, A.; Velasco, M. D.; Molina, P.; Evans, D. J. *Chem. Commun.* **2004**, 458–459.

(12) (a) Molina, P.; Vilaplana, M. J. *Synthesis* **1994**, 1197. (b) Arques, A.; Molina, P. *Curr. Org. Chem.* **2004**, *8*, 827.

(13) Alain, V.; Fort, A.; Brazoukas, M.; Chen, T.-H.; Blanchard-Desce, S. R.; Marder, S. R.; Perry, J. W. *Inorg. Chim. Acta* **1996**, *242*, 43–49.

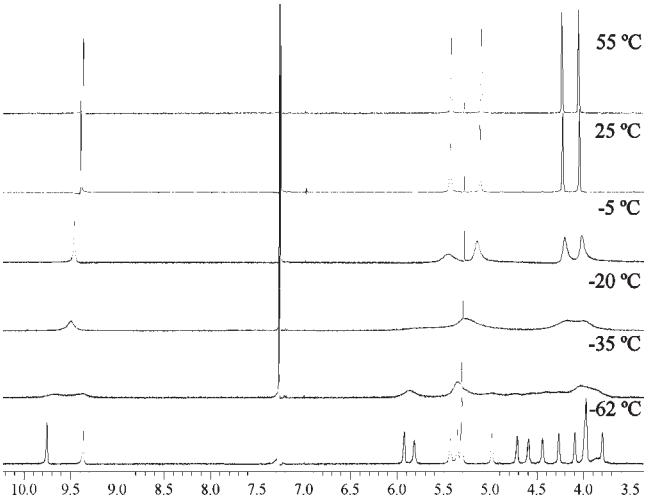

Figure 1. Evolution of ^{1}H NMR spectrum of the receptor **3** ($c = 5 \times 10^{-3}$ M, $CDCl_3$) with the temperature, showing its conformational exchange in solution.

these observations the first wave obtained for compound **3** is assigned to the oxidation of the ferrocene unit directly linked to the nitrogen atoms, whereas the second wave is due to the oxidation of the ferrocene linked to the methine units. The fact that the separation of the potential waves for compound **3** ($\Delta E_{1/2} = 510$ mV) is higher than the difference between compound **4** and **5** ($\Delta E_{1/2} = 290$ mV) is an indication that this separation is not only caused by the different environment of the ferrocene units but also by electronic interaction suffered by the second ferrocene unit upon oxidation of the first moiety indicating clearly the electronic communication existing in the molecule through the imine bridges.

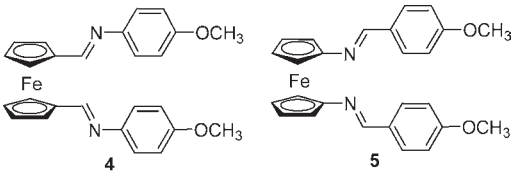

Block 2

Conformational Study by ^{1}H NMR. A temperature-dependent ^{1}H NMR experiment was carried out, to study the conformational behavior of compound **3** in solution (Figure 1). At −5 °C, a broadening of the peaks with respect to the room temperature (RT) spectra is clearly observed. At −62 °C a new pattern of peaks is observed, in which the signals of the compound are split into two peaks with similar intensities with a coalescence temperature of −25 °C. This experiment demonstrates the interconversion between two different conformers in solution, which must be very close in energy.

Indeed quantum chemical calculations provided the required structural and thermodynamical information, as two minima close in energy were found in the potential energy surface. The absolute minimum presents a C_s symmetry ($\mathbf{3}^{Cs}$) with both imine N atoms pointing to the same side of the molecule (Figure 2). By rotation around the outer linkages of one of the imine bridges, the structure of the other C_2-symmetry atropoisomer ($\mathbf{3}^{C2}$) can be reached through a rather low energetic transition state ($\mathbf{3}^{TS}$) accounting for the relatively low coalescence temperature found from the

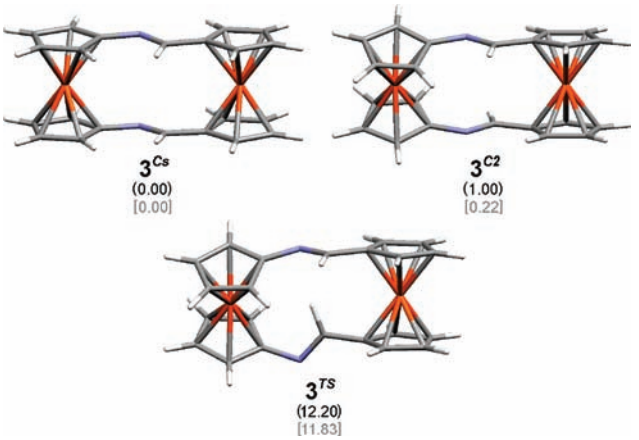

Figure 2. Calculated minima for compound **3** and the transition state ($\mathbf{3}^{TS}$) between them. In brackets their calculated relative Gibbs free energies (kcal·mol^{-1}) in $CHCl_3$ solution (black) and in the gas-phase (gray) are given.

NMR experiment. In addition, the low energetic difference calculated between both species would explain the comparable amounts of them present in the equilibrium (e.g., 59.4/40.6 in the gas-phase).

Spectroelectrochemistry and Study of the Conformational-Modulated Intramolecular Electron Transfer Process. To generate the mixed-valence species and study the intramolecular electron transfer process for the ferrocenophane **3** we generate the one electron oxidized species $\mathbf{3}^{+\cdot}$, derived from it either chemically or electrochemically. The chemical oxidation was performed with the appropriate amount of nitrosyl tetrafluoroborate, while the electrochemical oxidation was achieved by constant potential electrolysis, at 0.15 V and monitored by absorption spectroscopy. Stepwise Coulometric titration was performed on an about $c = 3.5 \times 10^{-3}$ M solution of compound **3** in CH_2Cl_2 using TBAHP as supporting electrolyte, and the absorption spectra were regularly recorded for different average number ($0 < n < 1$) of removed electrons. The most interesting feature, detected during the first-electron oxidation at 0.15 V occurring at the nitrogen linked ferrocene, is that two new bands appeared in the near-IR region: one intense band centered at $\lambda_{max} = 1519$ nm ($\nu_{max} = 6582$ cm^{-1}, $\varepsilon = 1577$ M^{-1} cm^{-1}) and a weaker and lower energy band at $\lambda_{max} = 2232$ nm ($\nu_{max} = 4480$ cm^{-1}, $\varepsilon = 447$ M^{-1} cm^{-1}) (Figure 3). Their intensities continuously grow until one electron is removed, that is, when the formation of $\mathbf{3}^{+\cdot}$ is completed. Furthermore, two well-defined isosbestic points at $\lambda = 540$ nm and $\lambda = 922$ nm are maintained during the course of the partial oxidation process. On removing the second electron at 0.8 V ($1 < n < 2$), the intensity of the two bands decrease until they disappear when the dication $\mathbf{3}^{2+}$ is completely formed which is indicative of the IET nature of the two bands.

The presence of several NIR bands in the spectrum of a mixed-valence complex is not uncommon, and their occurrence is generally explained by means of three different possible causes.[14,15] The first one could be the

(14) (a) Kober, E. M.; Goldsby, K. A.; Narayane, D. N. S.; Meyer, T. J. *J. Am. Chem. Soc.* **1983**, *105*, 4303–4309. (b) Lay, P. A.; Magnuson, R. H.; Taube, H. *Inorg. Chem.* **1988**, *27*, 2364–2371. (c) Laidlaw, W. M.; Denning, R. G. *J. Chem. Soc., Dalton Trans.* **1994**, 1987–1994.

(15) (a) Richardson, D. E.; Taube, H. *J. Am. Chem. Soc.* **1983**, *105*, 40–51. (b) Halpern, J.; Orgel, L. E. *Discuss. Faraday Soc.* **1960**, *29*, 32–41.

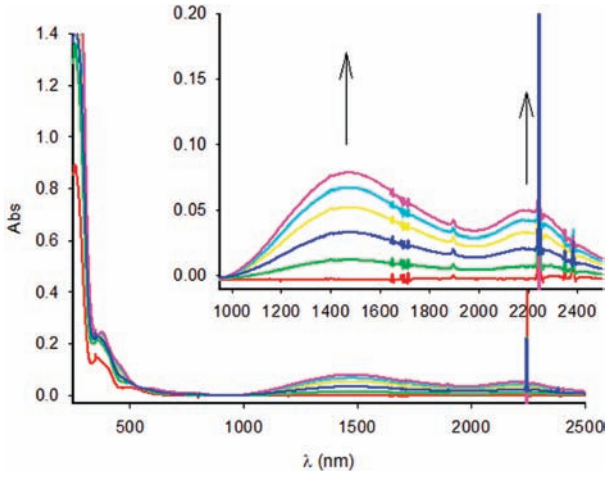

Figure 3. Evolution of UV−vis−NIR spectra during the course of the oxidation of compound **3** at 0.15 V in CH_2Cl_2 with $[(n\text{-}Bu)_4N]PF_6$ (0.15 M) as supporting electrolyte when $0 < n < 1$ electrons are removed. Arrows indicate absorptions that increase during the experiment.

presence of a strong spin−orbit coupling effect, which becomes important only for transition metals complexes of the third-row.[14] A second origin for these bands could be the presence of a double-exchange mechanism.[15] Finally, such multiple NIR bands might be also originated by the presence of a bridge with an accessible electronic state, that is, a bridge which is redox active.[16]

However, for compound **3** neither of the three explanations are adequate to justify the presence of the two NIR bands. First of all, to the best of our knowledge, the spin−orbit coupling effect has never been observed in ferrocene ligands. Moreover, the presence of double-exchange mechanism in addition to the superexchange is not a common cause for the presence of two different IET bands,[17] and the presence of a ligand-to-metal charge transfer (LMCT) process is very unlikely because the bands disappear in the double oxidized compound $\mathbf{3}^{2+}$. Thus, taking into account the Franck−Condon principle and the conformational behavior of **3**, demonstrated by low-temperature NMR experiments, a new origin for the presence of the two different absorption bands in the NIR can be considered. The proposed mechanism assigns each of the two bands to the two different observed conformers which are stable and can undergo IET processes. To ensure the conformational nature of these two bands the electro-generation of the monocation $\mathbf{3}^{+\cdot}$ was studied in three further solvents with different polarity: tetrahydrofuran (THF), EtOH, and *N*,*N*-dimethylformamide (DMF). Interestingly, when the oxidation of **3** is carried out in THF two well-defined transition bands appeared, whereas for the more polar solvents, EtOH and DMF, only one band is observed (Figure 4 and Table 1). The details of the two NIR transitions of $\mathbf{3}^{+\cdot}$ in the studied solvents are summarized in Table 1. Significantly, the high-energy band in the NIR shows a marked solvatochromism, being substantially red-shifted, $\Delta\lambda_{max} = 500$ nm, on moving from DMF to CH_2Cl_2. In accordance with the dielectric continuum model when the values of ν_{max} are plotted against $1/n^2 - 1/D$, where n is the refractive index and D the dielectric constant of the solvent, a linear relationship was found (see Supporting Information). The strong solvent dependence is therefore consistent with an IET origin of this band. The low-energy band in the NIR also shows a solvatochromism, although with a lower magnitude, in the two solvents in which it is observed pointing also to an IET origin.

The deconvolution of the experimental spectra of $\mathbf{3}^{+\cdot}$ in the NIR region, assuming Gaussian shapes in the wavenumber domain, allows an accurate determination of the position, width, and intensity of the two observed IET bands. These spectral parameters are relevant for the characterization of intramolecular electron-transfer phenomena occurring in $\mathbf{3}^{+\cdot}$.[18] The spectral parameters of the two bands present in the NIR, energy (ν_{max}), intensity (ε), and half-bandwidth ($\Delta\nu_{1/2}$), obtained by deconvolution of the experimental spectra as described above, have been used to determine the effective electronic coupling (V_{ab}) through the classical two-state Marcus−Hush theory.[19] Despite the simplicity of the Hush's theory, a good description of the phenomenon can be obtained.

According to the Robin and Day classification,[20] mixed-valence compounds are classified in three categories. Class I, in which the redox centers are completely localized and behave as separated entities. Class II, where an intermediate coupling between the mixed-valence centers exists. Class III, in which the system is completely delocalized and the redox centers show intermediate valence states. Recently, Meyer[21] defined borderline Class II/Class III systems, which exhibit both delocalized and localized behaviors. Hush theory[22] indicated that, for a Class II mixed-valence system with two unequivalent redox centers, the energy of the IET transition ν_{max} is given by $\nu_{max} = \lambda + \Delta G°$, where λ is the reorganization energy and $\Delta G°$ is the free energy difference between the initial and the final state after the electron transition. The reorganization energy is composed of two terms, $\lambda = \lambda_{in} + \lambda_{ext}$, that describe the contribution from the molecule itself, λ_{in}, and from the media, λ_{ext}, and which can be estimated from the plot of $1/n^2 - 1/D$ versus n, as previously commented. The reorganization energy is usually approximate to the separation $\Delta E_{1/2}$ of the redox potential of the processes centered on the isolated units involved in the electron transfer.[23] Thus, the magnitude of $\Delta G°$ can be obtained simply by converting the electrochemical value of $\Delta E_{1/2}$ into energy units. However, to estimate $\Delta G°$ more accurately, appropriate corrections on the values of the

(16) Nelson, S. F.; Ismagilov, R. F.; Powell, D. F. *J. Am. Chem. Soc.* **1998**, *120*, 1924–1925.

(17) (a) Paulson, B. P.; Miller, J. R.; Gan, W.-X.; Closs, G. *J. Am. Chem. Soc.* **2005**, *127*, 4860–4868. (b) Giacalone, F.; Segura, J. L.; Martín, N.; Ramey, J.; Guldi, D. M. *Chem.—Eur. J.* **2005**, *11*, 4819–4834. (c) Jordan, K. D.; Paddon-Row, M. N. *Chem. Rev.* **2002**, *92*, 395–410.

(18) The proportion of mixed valence species at half-oxidation (P), where $P = K_c^{1/2}/(2+K_c^{1/2})$, is generally used to compute the intensity of corrected spectra. The comproportionation constant K_c, which is related to the thermodimanic stability of the mixed-valence compound, of the equilibrium of comproportionation, $[Fe^{II}\text{-L-}Fe^{II}] + [Fe^{III}\text{-L-}Fe^{III}] \rightarrow 2[Fe^{II}\text{-L-}Fe^{III}]$, was calculated for **3** from the electrochemical data, resulting in a value of $K_c = 1107$ which yields values of P about 94.4%.

(19) Allen, G. C.; Hush, N. S. *Prog. Inorg. Chem.* **1967**, *8*, 357–389.

(20) Robin, M.; Day, P. *Adv. Inorg. Radiochem.* **1967**, *10*, 247–427.

(21) Chen, P.; Meyer, T. *J. Chem. Rev.* **1998**, *98*, 1439–1478.

(22) Hush, N. S. *Coord. Chem. Rev.* **1985**, *64*, 135–157.

(23) (a) Barlow, S. *Inorg. Chem.* **2001**, *40*, 7047–7053. (b) Albinati, A.; Fabrizi de Biani, F.; Leoni, P.; Marchetti, L.; Pasquali, M.; Rizzato, S.; Zanello, P. *Angew.Chem. Int. Ed.* **2005**, *44*, 5701–5705. (c) Santi, S.; Orian Durante, L. C.; Bisello, A.; Benetollo, F.; Croacini, L.; Ganis, P.; Ceccon, A. *Chem.—Eur. J.* **2007**, *13*, 1955–1968.

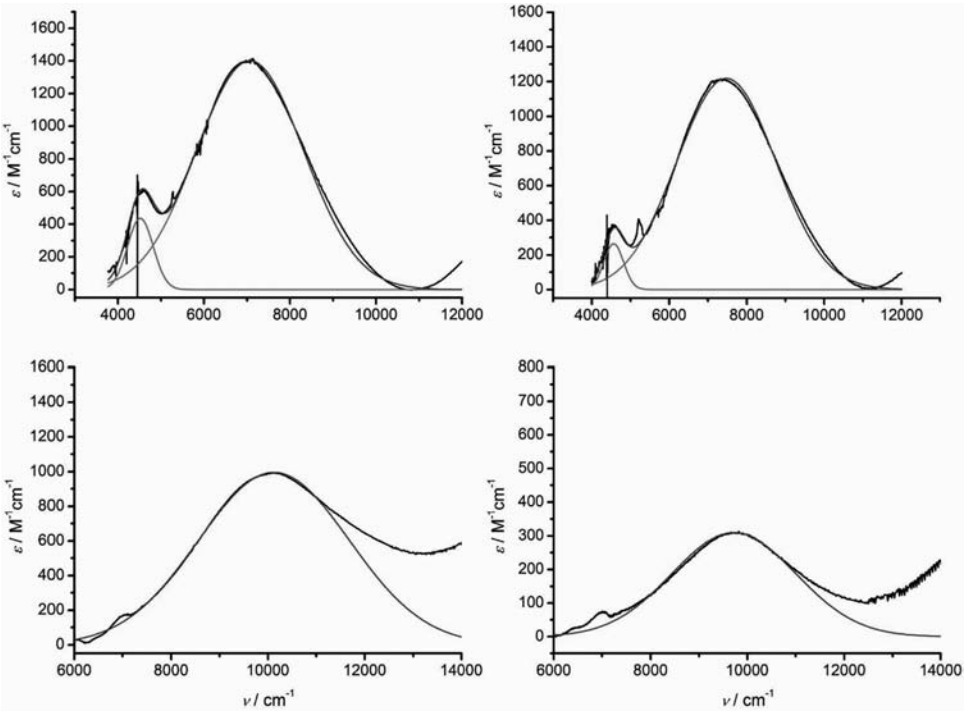

Figure 4. Deconvolution of the spectra of the mixed valence compound $\mathbf{3}^{+\cdot}$: Top/left, in CH_2Cl_2; Top/right, in THF; Bottom/left, in EtOH; Bottom/right, in DMF. Experimental data (black) were deconvoluted by means of Gaussian functions using molar absortivity versus wavenumbers. The sum of the deconvoluted spectra (blue) closely matches the lowest energy part of the experimental spectra.

Table 1. Spectroscopic Data Obtained of the Deconvoluted Spectra of the Mixed-Valence Compound $\mathbf{3}^{+\cdot}$

solvent	λ_{max} (nm)	ν_{max} (cm^{-1})	ε ($M^{-1}cm^{-1}$)	$\Delta\nu_{1/2exp}$[a] (cm^{-1})
CH_2Cl_2	1519, 2232	6582, 4480	1577, 447	3055, 691
THF	1435, 2203	6968, 4537	1314, 292	2946, 610
EtOH	1044	9574	1072	3975
DMF	1067	9366	369[b]	3550

[a] $\Delta\nu_{1/2}$ is the observed full width at half intensity of the band. [b] The low intensity of the band in this solvent is due in part to the decomposition of the mixed-valence compound $\mathbf{3}^{+\cdot}$; this value has to be taken as an apparent molar absortivity.

potentials of the redox centers present in compound **3** have to be made. The $\Delta E_{1/2}$, which is indicative of the metal−metal interaction, is no longer the difference between the redox potential between the two subsequent reversible redox waves of **3** ($\Delta E_{1/2}$ = 510 mV in CH_2Cl_2), but it is the difference between the redox potential of the reversible second wave of **3** and the redox potential of the reversible wave of the corresponding monometallic compound **4** ($\Delta E_{1/2}$ = 230 mV in CH_2Cl_2) leading therefore to a $\Delta G°$ value of 1855 cm^{-1}. The $\Delta G°$ values for $\mathbf{3}^{+\cdot}$ in the remaining solvents were determined as explained before and are shown in Table 2.

For the Class II regime, $\Delta\nu_{1/2theo}$ at RT and the electronic coupling V_{ab} are derived from the Hush equation $\Delta\nu_{1/2theo} = (2310\lambda)^{1/2}$ and $V_{ab} = (0.0205/d_{ab})(\varepsilon\nu_{max}\Delta\nu_{1/2})^{1/2}$, where d_{ab} is the diabatic metal−metal distance, which has been estimated from the Fe−Fe distance obtained in the theoretical calculations (d_{Fe-Fe} = 6.021/5.895/5.895 Å for the C_s isomer and d_{Fe-Fe} = 6.001/5.894/5.891 Å for the C_2 isomer, in the gas-phase and CH_2Cl_2 and DMF solutions, respectively). Additionally, the delocalization coefficient α, which is a parameter that quantifies the degree of valence delocalization in the ground state, can be calculated by using the equation $\alpha = V_{ab}/\nu_{max}$. The magnitude of the Γ parameter [$\Gamma = 1-(\Delta\nu_{1/2exp}/\Delta\nu_{1/2theo})$] has also been used alternatively to classify the mixed-valence systems. Values for this parameter in the range $0 < \Gamma < 0.1$ indicate the presence of a weakly coupled Class II systems while those in the range $0.1 < \Gamma < 0.5$ are typical for moderately coupled Class II systems. Finally a value such as $\Gamma = 0.5$ points out to a system at the transition between Class II and Class III and $\Gamma > 0.5$ for a Class III mixed-valence system.[24] The data for the two NIR bands observed for $\mathbf{3}^{+\cdot}$ and the calculated parameters by means of the Marcus−Hush theory are given in Table 2.

For the mixed-valence conformer of $\mathbf{3}^{+\cdot}$ showing the higher energy band, the comparison between $\Delta\nu_{1/2exp}$ and $\Delta\nu_{1/2theo}$ indicates that the experimental value is less than that predicted for a class II mixed-valence species. The localization versus delocalization is determined by the relative magnitudes of V_{ab} and λ being $V_{ab} \ll \lambda$ indicative that this mixed-valence conformer belongs to Class II. In addition, the values of the Γ parameter also indicate that this mixed-valence conformer is a weakly coupled Class II system. The magnitudes of the delocalization coefficient, α, are comparable to those found for ferrocene-ferrocenium systems with unsaturated bridging carbon atoms.[25] On the other hand, the sensitivity of this IET band to solvent variation is generally accepted as a criterion for distinguishing between localization or delocalization.[26] The strong solvent dependence of the higher-energy IET

(24) Brunschwig, B. S.; Sutin, N. *Coord. Chem. Rev.* **1999**, *187*, 233–254.
(25) (a) Venkatasubbaiah, K.; Doshi, A.; Nowik, I.; Herber, R. H.; Rheingold, A. L.; Jäkle, F. *Chem.—Eur. J.* **2008**, *14*, 444–458.
(26) (a) Creutz, C.; Chou, M. H. *Inorg. Chem.* **1987**, *26*, 2995–3000. (b) Nelson, S. F.; Konradsson, A. E.; Telo, J. P. *J. Am. Chem. Soc.* **2005**, *127*, 920–925. (c) Dinolfo, P. H.; Lee, S. J.; Coropceanu, V.; Brédas, J.-L.; Hupp, J. T. *Inorg. Chem.* **2005**, *44*, 5789–5797.

Table 2. Parameters Calculated for $3^{+\cdot}$ by Means of Marcus−Hush Theory

solvent	$\Delta G°$ (cm^{-1})	λ_{in} (cm^{-1})	λ_{ext} (cm^{-1})	λ (cm^{-1})	$\Delta\nu_{1/2theo}$ (cm^{-1})	$\Delta\nu_{1/2exp}$ (cm^{-1})	V_{ab} (cm^{-1})	α	Γ
CH_2Cl_2	1855	685	4042	4727	3304 2462	3055, 691[b]	603,[a]	0.092,[a]	0.08 0.72[b]
THF	1694	846	4428	5274	3490 2489	2946, 610[b]	556[a]	0.080,[a]	0.16 0.75[b]
EtOH	403	2137	7034	9171	4603	3975	684	0.071	0.14
DMF	1694	846	6826	7672	4210	3550	206	0.022	0.16

[a] Values for the conformer showing the low energy IET band were not estimated because the Marcus−Hush equations are not applicable. [b] These values of Γ are probably overestimated because of the graphical treatment which deal underestimates values for $\Delta\nu_{1/2exp}$.

band of $3^{+\cdot}$ provides an additional experimental confirmation for its assignment to a Class II system. The solvent-dependent analysis also allows the estimation of the internal and external reorganization energies (λ_{in} and λ_{ext}, respectively, see Table 2). The values of λ_{ext} obtained are, in all cases, higher than λ_{in} and solvent-dependent which is again in agreement with a Class II mixed-valence compound.[27] Finally, the calculated values for the reorganization energy λ for $3^{+\cdot}$, in the range of 5000−9000 cm^{-1}, are consistent with a weakly coupled Class II system.

In the conformer with the low energy IET band, that appears only in the less polar solvents (CH_2Cl_2 and THF), this band appears narrower and less intense than the previously discussed one. The lower intensity of this band is ascribable to the small amount of this conformer present in the equilibrium, as the theoretical calculations predict (vide infra). However, the origin of the narrower width of this band is not immediately clear, although differences between theoretical and experimental $\Delta\nu_{1/2}$ values are not uncommon. They often arise from system nonidealities with respect to the model.[28] However, although the values of Γ calculated could be graphically overestimated because of the small intensity of the band, the narrower aspect of the band suggest this conformer is a Class II/III borderline, which is supported by the lower dependence with the polarity of the solvent when changing from CH_2Cl_2 to THF. A Class III compound has been discharged because of the high electrochemical asymmetry, and the localized character of the orbitals have been calculated theoretically (vide infra).

It has been reported that stereochemical changes profoundly influenced the magnitude of the reorganizational energy contribution to the electron transfer barrier, and they are indeed manifested in the IET parameters of the system.[29] This trend in the relative intensities of the IET components has been observed for the diastereoisomeric forms which incorporate angular-bridging ligands, where the bidentate binding sites of the bridging ligands are angularly disposed.[30] In our close-related case, the different intensities of the two IET parameters provide an indication of inherent differences in the extent of orbital overlap between the donor and the acceptor orbitals in the atropoisomeric forms. In addition, these differences also could indicate that stereochemical factors such as different solvent and anion interactions with the atropoisomeric forms may also influence the intermetal electronic interaction.[3a] These results contrast with the CV experiments already commented in which only two well-defined reversible one-electron waves are present, which is indicative of only one specie in solution. However the time scale of CV is much slower, and it is expected that the two waves correspond to an averaged signal for the two atropoisomers.

To corroborate that the presence of the two IET bands are associated to the cyclic rigid architecture of compound **3**, and consequently to the existence of different conformers, the synthesis and a spectroelectrochemical study of the bis(ferrocenyl) derivative **6**, an acyclic analogue of compound **3** bearing a single imine bridge,[31] were carried out. As expected, the electrochemical oxidation of one ferrocene moiety causes the appearance of only one intervalence band in CH_2Cl_2 at λ_{max} = 1328 nm (ν_{max} = 7531 cm^{-1}) with $\Delta\nu_{1/2exp}$ = 3589 cm^{-1} and ε = 440 $M^{-1}\,cm^{-1}$, (see Supporting Information). Therefore, the Marcus−Hush parameters calculated for $6^{+\cdot}$ are V_{ab} = 375 cm^{-1}, α = 0.050, and Γ = 0.143 ($\Delta\nu_{1/2theo}$ = 4171 cm^{-1}) suggesting that this mixed-valence compound is of Class II. These results, in addition to others previously obtained with similar compounds,[10a,32] make unlikely the explanations previously exposed of a double-exchange mechanism or a band originated in the bridge and strongly corroborate that the cause of the presence of two different bands in the NIR is inherent to the relative rigid structure of ferrocenophane **3**. On the other hand, the presence of only one IET band for $3^{+\cdot}$ in the most polar solvents could be caused by a change in the conformational dynamics of the ferrocenophane.

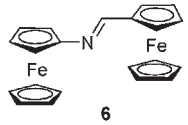

6

Block 3

Theoretical Study of the Conformationally Modulated IET. To support the experimental data pointing to a conformationally modulated IET process for compound $3^{+\cdot}$, a theoretical thorough inspection of the most stable structure and the conformational space of radical-cation

(27) Sierra, M. A.; Mancheno, M. J.; Vicente, R.; Gómez-Gallego, M. *J. Org. Chem.* **2001**, *66*, 8920–8925.
(28) (a) Elliot, C. M.; Derr, D. L.; Matyushov, D. V.; Newton, M. D. J. *Am. Chem. Soc.* **1998**, *120*, 11714–11726. (b) Curtis, J. C.; Meyer, T. J. *Inorg. Chem.* **1982**, *21*, 1562–1571. (c) Caballero, A.; Espinosa, A.; Tárraga, A.; Molina, P. *J. Org. Chem.* **2007**, *72*, 6924–6937 and references cited therein.
(29) D'Alessandro, D. M.; Keene, F. R. *Chem. Phys.* **2006**, *324*, 8–25.
(30) D'Alessandro, D. M.; Keene, F. R. *Chem.—Eur. J.* **2005**, *11*, 3679–3688.
(31) (a) Jones, S. C.; Barlow, S.; O'Hare, D. *Chem.—Eur. J.* **2005**, *11*, 4473–4481. (b) Masuda, Y.; Shimizu, C. *J. Phys. Chem. A* **2006**, *110*, 7019–7027. (c) Brunscbwig, B. S.; Ehrenson, S.; Sutin, N. *J. Phys. Chem.* **1987**, *91*, 4714–4723.
(32) (a) Otón, F.; Espinosa, A.; Tárraga, A.; Molina, P. *Organometallics* **2007**, *26*, 6234–6242. (b) Caballero, A.; García, R.; Espinosa, A.; Tárraga, A.; Molina, P. *J. Org. Chem.* **2007**, *72*, 1161–1173. (c) Lopez, J. L.; Tárraga, A.; Espinosa, A.; Velasco, M. D.; Molina, P.; Lloveras, V.; Vidal-Gancedo, J.; Rovira, C.; Veciana, J.; Evans, D. J.; Wurst, K. *Chem.—Eur. J.* **2004**, *10*, 1815–1826.

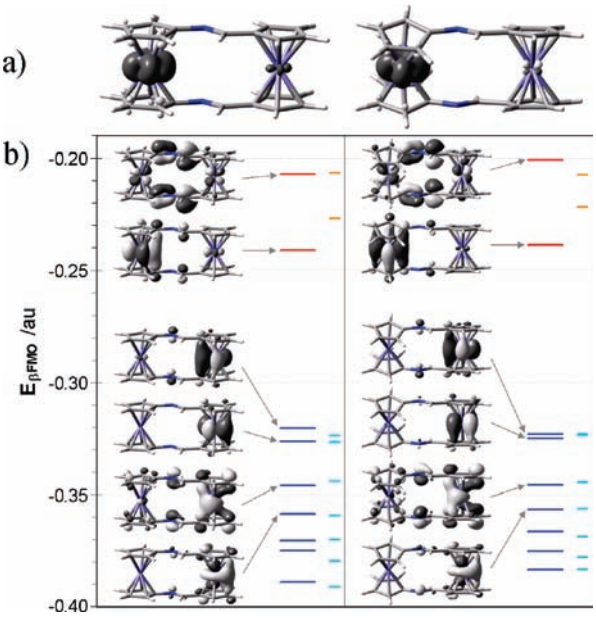

Figure 5. Calculated (a) spin distribution (0.005 isosurface) and (b) detailed scheme for the β-spin FMO (0.04 isosurface) involved in the NIR transitions for radical-cations $[\mathbf{3}^{qCs}]^{+\cdot}$ (left) and $[\mathbf{3}^{C2}]^{+\cdot}$ (right). Only four occupied (blue) and two unoccupied (red) orbitals are sketched. Short (cyan and orange) lines on right represent the energy of the corresponding FMO in the α-series.

$\mathbf{3}^{\cdot+}$ was performed. Each one of the two conformers found for the neutral precursor, $\mathbf{3}^{Cs}$ and $\mathbf{3}^{C2}$ were oxidized *in silico* giving rise to the corresponding radical-cations with *quasi-Cs*- $[\mathbf{3}^{qCs}]^{+\cdot}$ and *C2*-symmetry $[\mathbf{3}^{C2}]^{+\cdot}$. In spite of the fact that the ferrocene unit connected to the N atoms (Fc1) in **3** shows higher natural charge than Fc2 (q^{n}_{Fc1}/q^{n}_{Fc2} = 0.324/0.044 and 0.334/0.042 au, for $\mathbf{3}^{Cs}$ and $\mathbf{3}^{C2}$, respectively), the first electron oxidation takes place on Fc1 (Figure 5a) as expected by taking into account the higher energy of the uppermost Fe-centered 3d atomic orbital (AO) in this unit when compared to that on Fc2 ($\varepsilon^{u3d}_{Fe1}/\varepsilon^{u3d}_{Fe2}$ = −0.145/−0.153 and −0.154/−0.164 hartree, for $\mathbf{3}^{Cs}$ and $\mathbf{3}^{C2}$, respectively), in accordance to the electrochemical study on **3** and model compounds **4** and **5**. The corresponding transition state $[\mathbf{3}^{TS}]^{+\cdot}$ connecting both gas-phase optimized radical-cations was also located and characterized (ν = −192.17 cm^{-1}). The occurrence of metal to metal CT transitions in the studied MV compound can be rationalized in the light of frontier molecular orbitals (FMOs) qualitative analysis and time-dependent density functional theory (TD-DFT) calculations. The more significant feature in the molecular orbital (MO) diagram of MV compound $\mathbf{3}^{+\cdot}$ is the existence of a low-lying β-LUMO (singly occupied molecular orbital, SOMO; lowest unoccupied molecular orbital, LUMO; highest occupied molecular orbital, HOMO) consisting on a Fe1-centered $d_{x^2-y^2}$-type MO.[33] The lowest energy band in the NIR can arise as one or several optical transitions from the "neutral" Fe2-centered d-type MO (mainly HOMO, HOMO-1, and HOMO-3) to the above-mentioned SOMO (Figure 5b). Therefore it is assignable to a metal-to-metal Fe(II)→Fe(III) charge transfer (MMCT) transition which is X-polarized (i.e., in the bridge direction) and hence electric-dipole (ED) allowed.

The relatively high intensity of the MMCT bands in $\mathbf{3}^{\cdot+}$ could be explained by the high X-polarization of this electronic transition as a consequence of the low mixing between ferrocene units in both HOMOs and SOMO (Figure 5). Moreover, according to its lower HOMO/SOMO gap, $[\mathbf{3}^{qCs}]^{+\cdot}$ is expected to give a lower energy band in the NIR than isomer $[\mathbf{3}^{C2}]^{+\cdot}$. TD-DFT results show that only one slightly different LE band is expected in the NIR region for every one of the two conformers. These energies correspond to the highest doubly occupied MO to the SOMO transitions which are expected to occur at λ = 1228.2 nm (f = 0.057 au) for $[\mathbf{3}^{qCs}]^{+\cdot}$ and 1356.2 nm (f = 0.045 au) for $[\mathbf{3}^{C2}]^{+\cdot}$. Although the absolute values of the theoretically determined transition energies differ appreciably from the experimental data (Table 1), they provide information regarding the energetic sequence of the electronic transitions.

Very significant is the theoretical solvent dependence of the atropoisomeric equilibrium (Figure 6). According to our calculations in CH_2Cl_2 solution, as representative for poorly polar solvents, both $[\mathbf{3}^{qCs}]^{+\cdot}$ and $[\mathbf{3}^{C2}]^{+\cdot}$ atropoisomers are expected to coexist in observable amounts (computed 66.3/33.7 ratio) with a transition state (TS) barrier high enough to slow down their interconversion. For this reason, in CH_2Cl_2 the two NIR transitions corresponding to both species are observed experimentally, the lower energy band corresponding to the minor isomer (Figures 4 top/left). On the contrary in DMF solution, as model for polar solvents, the atropoisomeric equilibrium is enough shifted to the most stable radical-cation $[\mathbf{3}^{qCs}]^{\cdot+}$ in such an amount (computed 99.9/0.1 ratio) that the LE transition corresponding to that species is the only experimentally observed in the NIR (Figures 4 bottom/left). All these results strongly suggest the nature of the two IVCT bands found for **3** in CH_2Cl_2 and THF correspond to two different conformers in equilibrium in solution.

Bally, Tuczek and co-workers have carried more accurate calculations to obtain a good correspondence between experimental and theoretical results.[8c] With this aim we have used a comparable level of theory, the same BP86 "pure" functional but using an extensive basis set of triple-ζ quality with polarization (Def2-TZVP). We have even gone one step further and, being conscious of the critical character of solvent effects, we have also used the COSMO methodology during the geometry optimization step with the aid of the ORCA program package.[34] At this level, the TD-DFT calculation for the $[\mathbf{3}qC_s]^{+\cdot}$ isomer in CH_2Cl_2 predicts only one significant (with high oscillator strength f = 0.0976) band at λ = 1069.2 nm mainly corresponding to a HOMO-3→SOMO (with also some HOMO→SOMO contribution). The source for the second lower energy and less intense experimentally observed band is the only significant band in this region calculated for the other $[\mathbf{3}C_2]^{+\cdot}$ isomer, which is expected to be a bit less intense (f = 0.0772) and shifted to lower energies (λ = 1180.5 nm). This band originates from a different electronic transition mainly of HOMO→SOMO type. We believe that the different nature of the main NIR-transitions involved for every radical-cationic isomer could be one of the origins

(33) The coordinate system is oriented such that the x axis is along the intermetallic axis and the z axis is perpendicular to the Cp planes.

(34) Neese, F. *ORCA*, Version 2.7.0; University of Bonn: Bonn, Germany, 2009.

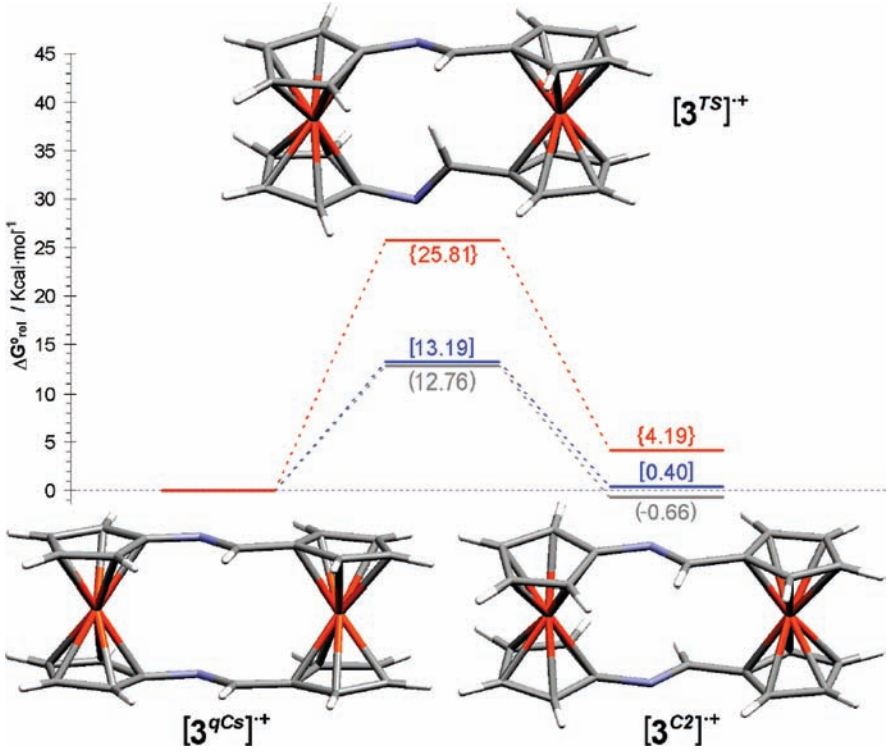

Figure 6. Atropoisomeric equilibrium calculated for radical-cations $3^{+\cdot}$. In brackets their calculated relative Gibbs free energies (kcal mol^{-1}) in the gas-phase (gray) and in CH_2Cl_2 (blue) and DMF (red) solutions.

of the experimentally obtained different widths for the two observed bands. Assuming the existence of roughly only one isomer in the equilibrium in DMF solution (Figure 6), the TD-DFT calculation for the $[\mathbf{3}qC_s]^{+\cdot}$ structure predicts the occurrence of only one (a bit less intense, $f = 0.0969$) band at $\lambda = 1073.4$ nm. In the case of the singly bridged radical-cation $\mathbf{6}^{\cdot+}$ only one configurational isomer is possible (although displaying a complex conformational dynamics), and only one transition is expected to occur in the NIR in CH_2Cl_2 solution ($\lambda = 1008.9$ nm, $f = 0.2840$). A more detailed explanation of these calculations can be found in the Supporting Information. These results support that each NIR band originates from a different conformer which are simultaneously present in the solution, making the presence of two bands in a single conformer very improbable.

Conclusions

The synthesis of a new [2.2]ferrocenophane, starting from 1,1′-bis(azido)ferrocene, as well as the study of their electrochemical, optical, and electronic properties have been carried out. The rigid and well-defined architecture of the prepared ferrocenophane made it possible to obtain a suitable model to study how conformational changes can induce modifications of the IET energy in the mixed-valence system. The mixed-valence compound $\mathbf{3}^{+\cdot}$, generated either electrochemically or chemically, displays two IET bands in the NIR region when measured in a poorly polar solvent, attributable to two different stable atropoisomers. Temperature and solvent control over the atropoisomeric equilibrium have been studied, both atropoisomers showing different energies for their IET and thus, exhibiting optical transitions of different nature (Class II and Class II/III behavior). Additionally, the theoretical TD-DFT calculations were carried out to support and explain the experimental results. To the best of our knowledge, this is the first example of a compound whose two conformers in equilibrium simultaneously cause the appearance of two clearly isolated metal-to-metal charge transfer (MMCT) bands in the NIR region of the spectrum offering a new point of view for the conformational modulation of intramolecular IET processes.

Experimental Section

General Information. All reactions were carried out using solvents which were dried by routine procedures. All melting points were determined on a Kofler hot-plate melting point apparatus and are uncorrected. IR spectra were determined as Nujol emulsions or films on a Nicolet Impact 400 spectrophotometer. UV−vis−NIR spectra were taken on a Varian Cary 5000 spectrophotometer. ^{1}H, ^{13}C, NMR spectra were recorded on a Bruker AC200, 300, or 400 MHz. The following abbreviations for stating the multiplicity of the signals have been used: s (singlet), bs (broad singlet), d (doublet), t (triplet), bt (broad triplet), m (multiplet), and q (quaternary carbon atom). Chemical shifts refer to signals of tetramethylsilane in the case of ^{1}H and ^{13}C NMR spectra. The EI mass spectra were recorded on a Fisons AUTOSPEC 500 VG spectrometer. Microanalyses were performed on a Carlo-Erba 1108 instrument. The cyclic voltammetric measurements were performed on a QUICELTRON potentiostat/galvanostat controlled by a personal computer and driven by dedicated software with a conventional three-electrode configuration consisting of platinum working and auxiliary electrodes and a SCE reference electrode. The experiments were carried out with a 10^{-3} M solution of sample in the appropriate solvent containing 0.1 M $[(n\text{-Bu})_4\text{N}]PF_6$ as supporting electrolyte. Deoxygenation of the solutions was achieved by bubbling nitrogen for at least 10 min, and the working electrode was cleaned after each run. The cyclic voltammograms were recorded with a scan rate increasing from 0.05 to 1.00 V s^{-1}. Ferrocene was used as an internal reference both for potential calibration and for reversibility criteria in all

the solvents used. Oxidations were performed by electrolysis in a three-electrode cell under argon using dry solvents and 0.15 M $[(n\text{-Bu})_4N]PF_6$ as supporting electrolyte. The progress of the oxidation was followed coulometrically (or chronoamperometrycally) with a 263A of EG&PAR potentiostat-galvanostat. The reference electrode and the counter electrode were separately immersed in the solvent containing the supporting electrolyte and isolated from the bulk solution by a glass fit. The working electrode was a platinum grid. UV−vis−NIR absorption spectra were regularly recorded by transferring a small aliquot of the solution contained in the electrochemical cell into a UV quartz cell for different average number of removed electrons.

Calculated geometries were fully optimized in the gas-phase with tight convergence criteria at the DFT level with the Gaussian 03 package[35] by using the standard B3LYP functional. The 6-311G** basis set was used for all atoms, adding diffuse functions on donor atoms (O, N, and Fe) (denoted as aug6-311G**). Ultrafine grids (99 radial shells and 590 angular points per shell) were employed for numerical integrations. From these gas-phase optimized geometries all reported data were obtained by means of single-point (SP) calculations. Energy values were computed at the same level and considering effects by using the Cossi and Barone's CPCM (conductor-like polarizable continuum model) modification[36] of the Tomasi PCM formalism.[37] Only those energies computed for the study of the atropoisomeric equilibrium in **3** and $\mathbf{3}^{\cdot+}$ are corrected for the zero-point vibrational energy. The same level of theory was used to perform the Natural Bond Orbital (NBO) population analysis, from which natural charges and AO energies were obtained. Bond orders were characterized by the Wiberg bond index (WBI)[38] and calculated with the NBO method as the sum of squares of the off-diagonal density matrix elements between atoms. TD-DFT calculations were performed at the current level of theory onto gas-phase optimized geometries.

Bis(methylidenamino)[2,2](1,1′′;1′,1′′′)ferrocenophane (3). To a solution of 1,1′-diformylferrocene (0.12 g, 0.54 mmol) in anhydrous toluene (130 mL) a solution of 1,1′-bis(triphenilfosforanilidenamino)ferrocene **2** (0.40 g, 0.54 mmol) in the same solvent (100 mL) was added at RT and under nitrogen. The solution was refluxed and stirred overnight, and the solvent removed under vacuum to give a residue which was chromatographed on a silica gel column, using 9:1 CH_2Cl_2/CH_3OH as eluent to give **3** (R_f = 0.8) in 72% yield, which was crystallized from CH_2Cl_2/Et_2O (2:1). Physical data of **3**: mp 237−240 °C (d). Anal. Calcd for $C_{22}H_{18}Fe_2N_2$: C, 62.56; H, 4.27 ; N, 6.64 . Found: C, 62.70; H, 4.31 ; N, 6.65. ν_{max} (Nujol)/cm^{-1} 1612, 1035, 937, 822, 732. δ_H (200 MHz; $CDCl_3$; Me_4Si) 4.07 (4H, s, Fc), 4.24 (4H, s, Fc), 5.12 (4H, s, Fc), 5.44 (4H, s, Fc), 9.39 (2H, s, CH=N). [1] δ_C (100.4 MHz; $CDCl_3$; Me_4Si): 64.60 (CH, Cp), 67.10 (CH, Cp) 69.70 (CH, Cp), 70.40 (CH, Cp), 80.80 (q, Cp), 102.20 (q, Cp), 165.60 (CH=N). *m*/*z* (EI) 422 (M^+, 100), 357 (15), 343 (13), 211 (18).

1,1′-Bis[(4-methoxyphenylimino)methyl]ferrocene (4). To a solution of 1,1′diformylferrocene (0.100 g, 0.413 mmol) and sodium sulfate (5 g) in dry CH_2Cl_2 (10 mL), a solution of 4-methoxyaniline (0.100 g, 0.826 mmol) in the same solvent was added at RT, under nitrogen. The mixture was stirred for 8 h, and then the solvent was partially removed under vacuum giving rise to the precipitation of a red solid which was recrystallized in CH_2Cl_2/dimethylether (1:1) to yield 0.177 g; 95%. Physical data of **4**: mp 154−157 °C. Anal. Calcd. for $C_{26}H_{24}FeN_2O_2$: C, 69.04; H, 5.35; N, 6.19. Found: C, 68.90; H, 5.19; N, 5.99. ν_{max} (Nujol)/cm^{-1} 1618, 1577, 1507, 1293, 1248, 1216, 1186, 1162, 1108, 1034, 829. δ_H (300 MHz; $CDCl_3$; Me_4Si) 8.27 (2H, s, imina), 7.08 (4H, d, *J* 8.7 Hz, Ar), 6.83 (4H, d, *J* 8.7 Hz, Ar), 4.85 (4H, t, *J* 1.8 Hz, Fc), 4.50 (4H, t, *J* = 1.8 Hz, Fc), 3.81 (6H, s, CH_3). δ_C (75.3 MHz; $CDCl_3$; Me_4Si) 158.4 (q, imine), 157.7 (q, Ar) 145.3 (q, Ar), 121.7 (CH, Ar), 114.2 (CH, Ar), 82.0 (q, Fc), 71.9 (CH, Fc), 69.8 (CH, Fc), 55.4 (CH_3). *m*/*z* (FAB^+) 453 (M^++1, 100).

1,1′-Bis(4-methoxybencilidenamino)ferrocene (5). To a solution of 1,1′-bis(azido)ferrocene (0.100 g, 0.370 mmol) in dry THF (30 mL), tributhylphosphine (0.307 mL) was added at RT and under nitrogen. After stirring the solution for 1 h, a solution of 4-methoxybenzaldehyde in the same solvent (10 mL) was added, and the mixture was refluxed for 6 h. Then the solution was allowed to cool down, and the solvent was partially removed under vacuum. Finally, after the addition of *n*-hexane (20 mL) a red solid precipitated, which was recrystallized in CH_2Cl_2/dimethylether (1:1) to yield 0.117 g; 70%. Physical data of **5**: mp 147−150 °C. Anal. Calcd. for $C_{26}H_{24}FeN_2O_2$: C, 69.04; H, 5.35; N, 6.19. Found: C, 68.89; H, 5.48; N, 6.27. ν_{max} (Nujol)/cm^{-1} 1607, 1575, 1311, 1258, 1168, 1032, 831. δ_H (400 MHz; $CDCl_3$; Me_4Si) 8.37 (2H, s, imine), 7.54 (4H, d, *J* 8.4 Hz, Ar), 6.78 (4H, d, *J* 8.4 Hz, Ar), 4.58 (4H, br s, Fc), 4.26 (4H, br s, Fc), 3.84 (6H, s, CH_3). δ_C (75.3 MHz; $CDCl_3$; Me_4Si) 161.4 (q, imine), 157.7 (q, Ar), 129.6 (q and CH, Ar), 113.9 (CH, Ar), 105.8 (q, Fc), 68.1 (CH, Fc), 64.0 (CH, Fc), 55.3 (CH_3). *m*/*z* (FAB^+) 453 (M^++1, 100).

Acknowledgment. We gratefully acknowledge the financial support from MICINN-Spain, Projects CTQ2008-01402 and "Eje C-Consolider" EMOCIONa (CTQ2006-06333/BQU), from the Fundación Séneca (Agencia de Ciencia y Tecnología de la Región de Murcia), project 04509/GERM/06 (Programa de Ayudas a Grupos de Excelencia de la Región de Murcia, Plan Regional de Ciencia y Tecnología 2007/2010), from the Generalitat de Catalunya, AGAUR Grant 2009SGR-00516), from the CIBER de Bioingeniería, Biomateriales y Nanomedicina (CIBER-BBN is an initiative funded by the VI National R&D&i Plan *2008-2011, Iniciativa Ingenio 2010, Consolider Program, CIBER Actions* and financed by the Instituto de Salud Carlos III with assistance from the *European Regional Development Fund*.), Spain and from the Juan de la Cierva program (MICINN).

Supporting Information Available: ^{1}H and ^{13}C NMR spectra, UV−vis−NIR and electrochemical data and spatial coordinates of calculated molecular geometries. This material is available free of charge via the Internet at http://pubs.acs.org.

(35) Frisch, M. J.; Trucks, G. W.; Schlegel, H. B.; Scuseria, G. E.; Robb, M.; Cheeseman, J. R.; Montgomery, J. A.; Vreven, J. A.; Kudin, K. N.; Burant, J. C.; Millam, J. M.; Iyengar, S. S.; Tomasi, J.; Barone, V.; Mennucci, B.; Cossi, M.; Scalmani, G.; Rega, N.; Petersson, G. A.; Nakatsuji, H.; Hada, M.; Ehara, M.; Toyota, K. ; Fukuda, R.; Hasegawa, J.; Ishida, M.; Nakajima, T.; Honda, Y.; Kitao, O.; Nakai, H.; Klene, M.; Li, X.; Knox, J. E.; Hratchian, H. P.; Cross, J. B.; Adamo, C.; Jaramillo, J; Gomperts, R.; Stratmann, R. E.; Yazyev, O.; Austin, A. J.; Cammi, R.; Pomelli, C.; Ochterski, J. W.; Ayala, P. Y.; Morokuma, K.; Voth, G. A.; Salvador, P.; Dannenberg, J. J.; Zakrzewski, V. G.; Dapprich, S.; Daniels, A. D.; Strain, M. C.; Farkas, O.; Malick, D. K.; Rabuck, A. D.; Raghavachari, K.; Foresman, J. B.; Ortiz, J. V.; Cui, Q. ; Baboul, A. G. ; Clifford, S. ; Cioslowski, J.; Stefanov, B. B.; Liu, G.; Liashenko, A.; Piskorz, P.; Komaromi, I.; Martin, R. L.; Fox, D. J.; Keith, T.; Al-Laham, M. A.; Peng, C. Y.; Nanayakkara, A.; Challacombe, M.; Gill, P. M. W.; Johnson, B.; Chen, W.; Wong, M. W.; Gonzalez, C.; Pople, J. A. *Gaussian 03*, Revision B.03; Gaussian, Inc.: Wallingford, CT, 2004.

(36) (a) Barone, V.; Cossi, M. *J. Phys. Chem. A* **1998**, *102*, 1995–2001. (b) Cossi, M.; Rega, N.; Scalmani, G.; Barone, V. *J. Comput. Chem.* **2003**, *24*, 669–681.

(37) (a) Miertus, S.; Scrocco, E.; Tomasi, J. *J. Chem. Phys.* **1981**, *55*, 117–129. (b) Cammi, R.; Mennucci, B.; Tomasi, J. *J. Phys. Chem. A* **2000**, *104*, 5631–5637.

(38) Wiberg, K. *Tetrahedron* **1968**, *24*, 1083–1096.